La 3.5 Ru 4.0 O 13 Perovskite type Catalyst for Carbon Monoxide and Hydrocarbon Oxidation

9 AUTHORS, INCLUDING:

Nitin Labhsetwar
National Environmental Engineering Resea…
105 PUBLICATIONS **2,188** CITATIONS

SEE PROFILE

Pradeep Doggali
14 PUBLICATIONS **143** CITATIONS

SEE PROFILE

Satish K. Lokhande
National Environmental Engineering Resea…
6 PUBLICATIONS **93** CITATIONS

SEE PROFILE

Sadhana Rayalu
National Environmental Engineering Resea…
115 PUBLICATIONS **2,230** CITATIONS

SEE PROFILE

Combustion of volatile organic compounds over Cu–Mn based mixed oxide type catalysts supported on mesoporous Al_2O_3, TiO_2 and ZrO_2

Pradeep Doggali [a], Y. Teraoka [b], P. Mungse [a], Irfan K. Shah [c], S. Rayalu [a], Nitin Labhsetwar [a],*

[a] National Environmental Engineering Research Institute(CSIR-NEERI), Nehru Marg, Nagpur 440020, India
[b] Department of Energy and Material Sciences, Faculty of Engineering Sciences, Kyushu University, Kasuga, Fukuoka 816-8580, Japan
[c] Department of Civil Engineering, Indian Institute of Technology (IIT) Delhi, Hauz Khas, New Delhi 16, India

ABSTRACT

A series of supported Cu–Mn based catalysts have been synthesized using three different supports mesoporous Al_2O_3, mesoporous TiO_2 and mesoporous ZrO_2. Cu–Mn precursors were incorporated on mesoporous supports using wet impregnation method. These catalyst supports were prepared by templating method using a natural biopolymer namely, chitosan. The catalytic activity for benzene and acetaldehyde combustion was studied for these catalysts. The synthesized catalysts have been characterized by XRD, BET-SA, O_2-TPD and H_2-TPR in a view of material characterization, as well as to investigate the mechanistic aspects of catalytic reactions. The bimetallic supported catalysts follow the activity sequence—Cu–Mn/TiO_2 > Cu–Mn/ZrO_2 > Cu–Mn/Al_2O_3 for both the reactions studied. These results interestingly show, that the catalytic activity is dependent on the support used, however, quite independent of the surface area of these supports. The better activity of TiO_2 and ZrO_2 based catalysts is likely due to their redox properties. The existence of low temperature peaks in both O_2-TPD and H_2-TPR explain better redox properties as well as catalytic performance of TiO_2 and ZrO_2 supported catalysts as compared to those Al_2O_3 supported mixed oxides.

1. Introduction

Volatile organic compounds (VOCs) have high vapour pressure under normal atmospheric conditions and therefore, can be easily vaporized [1]. VOCs include a variety of different organic compounds including alcohols, ethers, esters, aromatics, chlorinated hydrocarbons and odorous compounds containing sulphur [2]. The major sources of VOCs are the paint industry, building materials, automobile exhaust, combustion exhaust, industrial off gases, personal care products as well as a range of other sources [3]. VOCs are often toxic [4] and also responsible for the formation of photochemical ozone [5] as well as secondary aerosols in urban air [6]. Therefore, removal of VOCs from ambient air and controlling VOC emission at source has now been deemed as crucial for environmental and health point of view. Although various types of air purification techniques such as adsorption and combustion processes have been developed and widely used for hazardous air pollutant removal, they are often not suitable for the removal of diluted pollutants [7]. The use of catalytic combustion allows decreasing the temperatures (<600 °C) to obtain complete combustion of organic compounds as compared to thermal processes

(>1000 °C) [8]. In addition, the cleaning efficiencies can be over 95%, which is especially important for malodorous VOCs since they are odorous at very low concentrations [9]. The lowering of reaction temperatures leads to several advantages in terms of environmental impact by minimizing secondary pollutants as well as energy saving and reduction of fuel costs [10].

Cu and Mn based oxides are the potential candidates for many catalytic reactions, environmental importance [11–17]. The well-known Cu–Mn mixed oxide in the form of hopcalite ($CuMn_2O_4$) has been used for ambient CO oxidation, especially in mining industries. Recently, Christopher Jones et al. studied the effect of calcination on the catalytic CO oxidation activity of Cu–Mn mixed oxide ($CuMnO_x$). They observed that aging time does not influence the catalytic activity significantly, when the catalyst is synthesized by co-precipitation method, and efficient CuMnOx catalysts can be produced at an optimum calcination temperature of 410 °C [18]. One of the advantages to use these catalysts is their low-cost. However; developing a suitable support for the Cu–Mn based catalysts adds to their potential, while use of catalyst support is often necessarily required for the final application. Generally the activity of catalytically active component depends upon both chemical and physical properties of support used, such as chemical composition, crystal structure and crucially on the porosity, particle size and surface area. Therefore, several efforts have been focused on tailoring the pore size and external morphology of supports in a view to

improve the catalytic properties of different catalysts dispersed on them. Li et al. [19] demonstrated high activity of Cu–Mn mixed oxides with mesoporous MCM-41 support for toluene combustion. Usually Al_2O_3, TiO_2 and ZrO_2 are considered to be thermally stable supports with reasonably good chemical stability and low cost. Extensive studies are therefore reported on transition metals supported on Al_2O_3, TiO_2 and ZrO_2 for their possible environmental applications [20–23].

Alumina mainly in its γ-form is the most commonly used catalyst support for a variety of applications. It is an inexpensive and reasonably stable support materials, which can be processed easily. High surface area can be achieved with alumina, which is useful for many gas phase catalytic reactions requiring high space velocities. Many researchers have also investigated the catalytic properties of TiO_2, as it is a promising reducible semiconductor metal oxide support with excellent stability. TiO_2 has been frequently demonstrated as a useful support as well as a photocatalyst for many reactions to decompose a variety of organics and other compounds [24]. ZrO_2 is also reported to be an active support for various combustion reactions. The anionic vacancies, even in small amount, leads to better oxygen mobility in ZrO_2 lattice [25,26]. It is an added advantage to make these supports in mesoporous form, thereby improving their surface area and pore characteristics, which are likely to result in improved mass transfer and reactant contacts in catalytic reactions. An abundantly available, low cost, natural biopolymer, chitosan was used as a template to synthesize these supports. Chitosan, copolymer of 2-amino-2-deoxy-D-glucopyranose and 2-acetamido-2-deoxy-D-glucopyranose, is N-de-acetylated product of chitin, and is the second most abundant natural polysaccharide in the ecosphere after cellulose. Both chitin and chitosan are of great interest because of their unique combination of properties, like biodegradability, biocompatibility and bioactivity, in addition to attractive physical and mechanical properties. It has been reported that chitosan has the higher metal coordinating ability as compared to other natural polymers [27]. In a recent article, we reported the catalytic behaviour of Cu–Mn supported Al_2O_3, TiO_2 and ZrO_2 for CO and PM oxidation reactions [28]. The encouraging results obtained with these catalysts motivated us to further investigate these catalysts for benzene and acetaldehyde combustion. The aim of the present investigation is to develop appropriate support with Cu–Mn mixed oxide system for the oxidation of benzene and acetaldehyde for their possible application in control of these VOCs emissions in indoor environment.

2. Experimental

2.1. Materials

All the reagents used for experimental work were of analytical reagent grade. Acetic acid, ammonia, aluminium nitrate, zirconyl nitrate, cupric acetate and manganese acetate were obtained from Merck India Ltd. Chitosan was procured from Chemchito India. Titanium isopropoxide was obtained from Acros India Ltd.

2.2. Methods

Mesoporous Al_2O_3 was synthesized following a similar procedure as reported elsewhere [29] and later applied for the synthesis of TiO_2 and ZrO_2 in our group [28–30]. The supports thus obtained were ground into powder, homogenised and used for the synthesis of supported catalysts. Aqueous equimolar solutions of the stoichiometric quantity of $Cu(CH_3COO)_2$ and $Mn(CH_3COO)_2$ were used to prepare mixed metal solution in deionized water. Catalysts were synthesized by targeted loading of 8 wt% Cu and 8 wt% Mn on mesoporous Al_2O_3, TiO_2 and ZrO_2 supports. The mixture of support and metal acetate solutions were stirred in a beaker for 3 h at 60 °C. Metal impregnated supports were then dried in an oven at 110 °C for 4 h. The dried mass thus obtained was again ground, homogenised and calcined at 400 °C in a furnace for 5 h.

2.3. Characterization

XRD patterns were recorded on a Rigaku Rint-220HF diffractometer, operated at 40 kV and 50 mA with monochromator, and using Cu Kα radiation (λ = 0.15418 nm). Indexing of XRD peaks was done, by using the JCPDS database for the respective phases. Surface area was measured by nitrogen adsorption using the automatic gas adsorption apparatus BELSORP 28SA (produced by Nippon Bell Co.) and evaluated by following BET method. The samples were pre-treated at 300 °C before the nitrogen adsorption experiments. Elemental analysis of the catalytic materials was carried out using PerkinElmer ICP-OES 4100 BV instrument to assess the content of copper and manganese present. The H_2-TPR and O_2-TPD analysis were performed in a Thermo-Quest TPD/R/O 1100 analyzer, equipped with a TCD detector. For H_2-TPR test, the quartz tube reactor was loaded with100 mg sample in powder form. It was pre-treated in He flow by heating the catalyst from room temperature to 400 °C for 30 min (10 mL/min, STP) and cooled to ambient under helium flow (10 mL/min, STP). The reduction was performed by flowing 5% hydrogen diluted in helium. The sample temperature was raised at 10 °C/min till 400 °C under 5% H_2/He (10 mL/min, STP) flow. The amount of hydrogen consumed in TPR was quantitatively measured by a thermal conductivity detector (TCD). In the similar way, temperature-programmed oxygen desorption (TPD) was performed. Prior to each run, the catalyst was heated up to 400 °C under the helium flow (30 N mL/min). After 30 min of isothermal heating at this temperature, the sample was cooled to 25 °C in air flow. Afterwards, helium was fed to the reactor at 10-mL/min-flow rate for 1 h at room temperature, in order to purge out any excess oxygen. The catalyst was then heated up to 400 °C at a constant heating rate of 10 °C/min under the same helium flow, and O_2 desorbed during the heating was determined to study the TPD pattern. CHN analysis was carried out on a Shimadzu Elementer. The copper and manganese contents of materials were determined using ICP-OES technique (PerkinElmer, Model Optima 4100DV). Blank experiments were conducted throughout the studies and majority of the experiments were repeated thrice and it was observed that the experimental error was within ±2%. The samples were dissolved in acid before the analysis.

2.4. Evaluation of catalytic activity

Catalytic activity of all the synthesized catalysts was investigated for benzene and acetaldehyde combustion (oxidation). The steady state, fixed bed gas evaluation assembly equipped with a quartz reactor, precise mass flow controllers and heating system was used in the present study. 100 mg powdered catalyst was loaded in a fixed bed quartz reactor. Catalysts were pre-treated in He flow at 200 °C for 1 h. The reactant gas mixture of 900 ppm benzene, 10% O_2 and He balance was used for benzene combustion while, 500 ppm acetaldehyde, 10% O_2 and balance He was used for the combustion of acetaldehyde. The exit gas stream was analyzed by a Shimadzu Gas chromatograph using a capillary column for benzene combustion and Porapack-N column for the combustion of acetaldehyde using FID and TCD detector, respectively. A schematic of the experimental setup is given in Fig. 1.
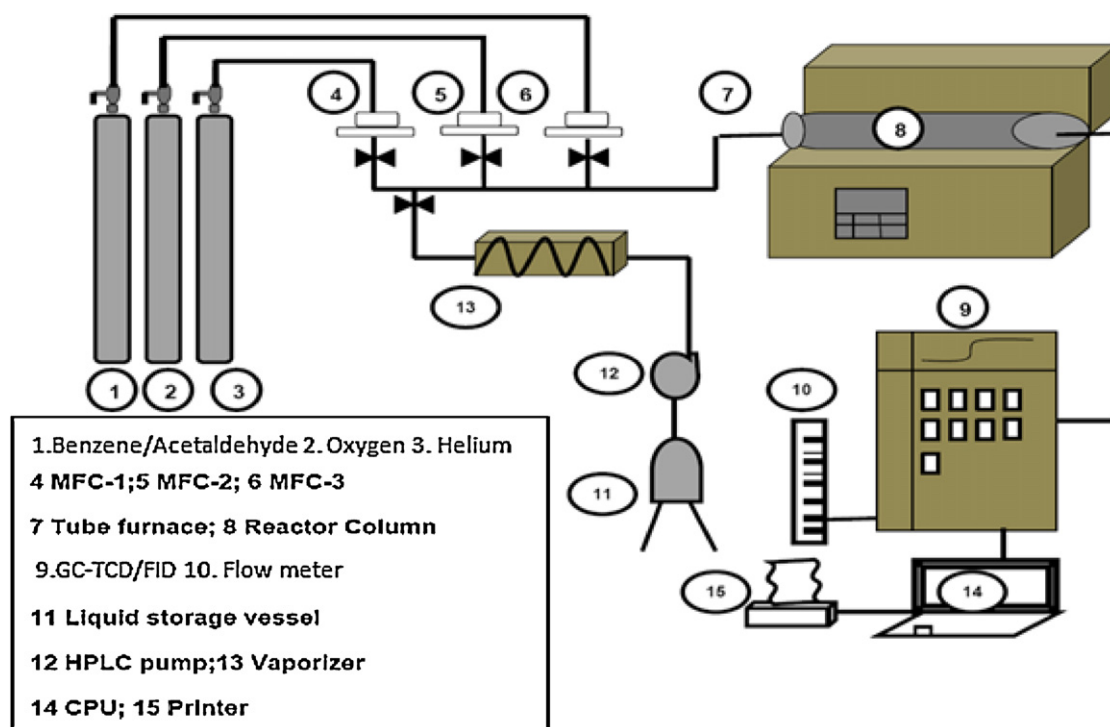
Fig. 1. Schematic of the experimental setup.

3. Results and discussion

The copper and manganese contents of synthesized Cu–Mn/Al$_2$O$_3$, Cu–Mn/TiO$_2$ and Cu–Mn/ZrO$_2$ was determined by digesting the Cu–Mn/Al$_2$O$_3$, Cu–Mn/TiO$_2$ and Cu–Mn/ZrO$_2$ compounds in aquaregia and analyzing by using ICP-MS technique. The observed results (Table 1) for Cu and Mn contents for catalytic materials substantiate the incorporation of targeted amount of copper and manganese on Al$_2$O$_3$, TiO$_2$ and ZrO$_2$.

The catalysts were characterized for their structure by X-ray powder diffraction analysis. Figs. 2–4 illustrates the XRD patterns for mesoporous Al$_2$O$_3$, TiO$_2$, ZrO$_2$, Cu–Mn/Al$_2$O$_3$, Cu–Mn/TiO$_2$ and Cu–Mn/ZrO$_2$ catalysts. XRD analysis suggests the formation of alumina phase with presence of the characteristic XRD peaks for γ-Al$_2$O$_3$ phase in the synthesized meso-alumina sample [29]. The synthesized meso-titania corresponds to TiO$_2$ anatase phase [30]. Patterns correspond to the tetragonal phase was observed in the synthesized mesoporous ZrO$_2$ sample [28].

The low angle peaks (1–3°) characteristic of ordered mesoporous structure were not observed [27]. This implies that the ordered mesoporous structure is not formed for all the three synthesized supports. The predominant crystalline chitosan peaks at 2θ values 8°, 20° and 29° were also not observed [27], which confirm the elimination of organic matter from the oxides formed. X-ray diffraction analysis of supported catalysts suggests no change in diffraction pattern after incorporation of Cu–Mn oxide on different supports, prepared by calcination at 400 °C. This could be because of small crystal sizes of the Cu–Mn species, as well as their good dispersion on support materials.

Results pertaining to BET surface area and pore size as determined by BJH method for the synthesized catalysts are presented in Table 2. The surface area results for synthesized mesoporous Al$_2$O$_3$, TiO$_2$, ZrO$_2$ are observed to be 312 m^2/g, 130 m^2/g and 34.9 m^2/g, respectively. The pore sizes of these catalysts are observed as 4.2 nm, 3.2 nm and 3.5 nm, respectively. These results clearly demonstrate that the investigated supports are mesoporous in nature and possess high surface area except that of mesoporous zirconia. However, the surface area of synthesized mesoporous zirconia was observed to be much higher as compared that of commercially available zirconia (HIMEDIA chemicals (14 m^2/g)). The results also indicate that surface area and pore size of the supports have been slightly decreased after Cu–Mn incorporation (150.9 m^2/g for Al$_2$O$_3$, 92.5 m^2/g for TiO$_2$ and 28.5 m^2/g for ZrO$_2$). For mesoporous alumina the pore size was observed to be 4.2 nm, which has been decreased to 3.4 nm after the impregnation of Cu–Mn mixed oxides. Similarly, in case of mesoporous TiO$_2$ and ZrO$_2$, the pore size has been decreased from 3.2 nm to 2.9 nm and 3.5 nm to 2.4 nm following the impregnation of Cu–Mn mixed oxides on these supports. This pore size and surface area results are in line with the pore volume results of the synthesized catalysts.

Table 1
ICP analysis results for Cu and Mn content of mesoporous Al$_2$O$_3$, mesoporous TiO$_2$ and mesoporous ZrO$_2$.

Sample	mg of metal/g of support
Cu–Mn/Al$_2$O$_3$	78 Cu–77 Mn/Al$_2$O$_3$
Cu–Mn/TiO$_2$	77 Cu–78 Mn/ZrO$_2$
Cu–Mn/ZrO$_2$	78 Cu–77 Mn/TiO$_2$

Table 2
Surface area pore size and pore volume results for mesoporous Al$_2$O$_3$, Cu–Mn/Al$_2$O$_3$, mesoporous TiO$_2$, Cu–Mn/TiO$_2$, mesoporous ZrO$_2$ and Cu–Mn/ZrO$_2$.

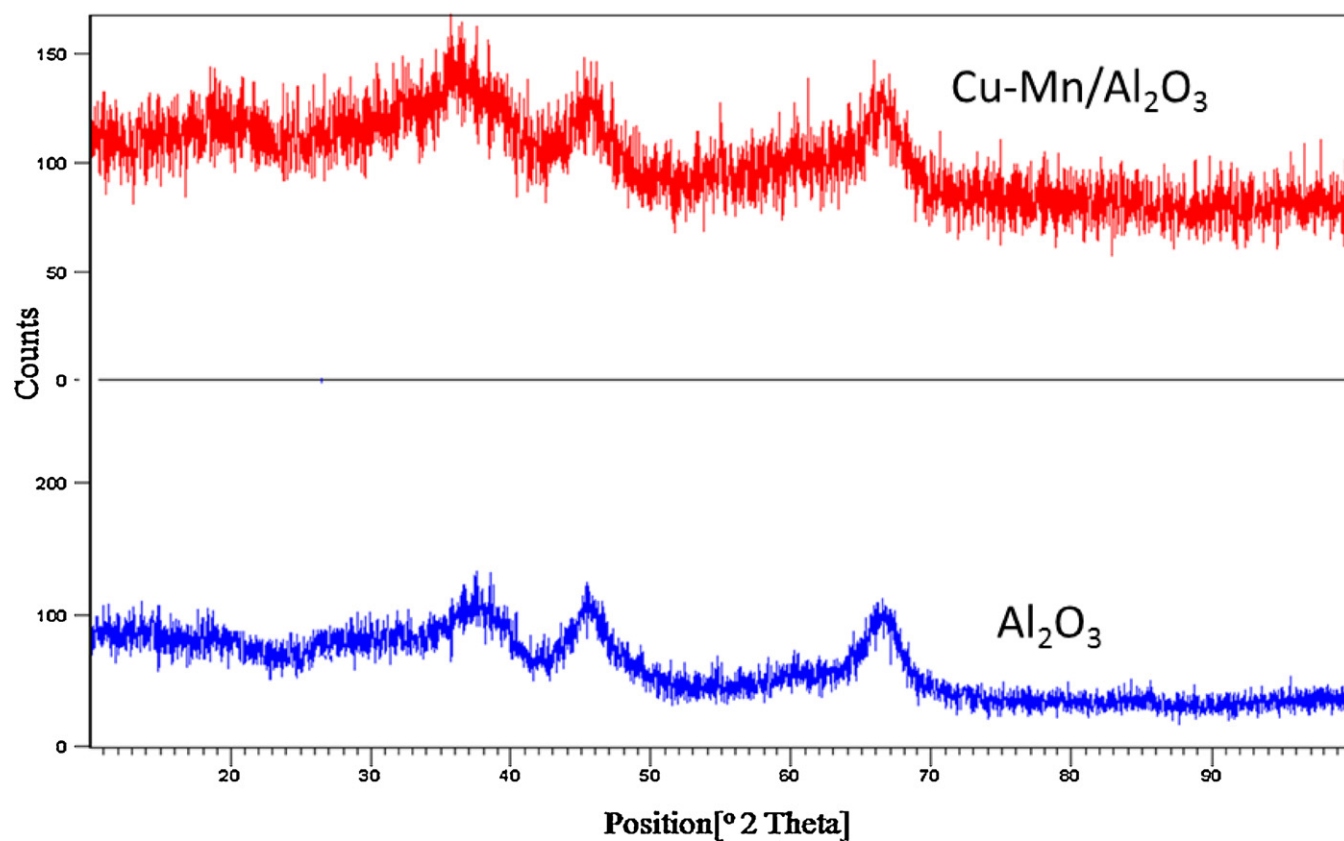| Sample	BET-surface area (m^2/g)	Pore diameter (nm)	Pore volume (cm^3/g)
Mesoporous Al$_2$O$_3$	312	4.2	0.36
Cu–Mn/Al$_2$O$_3$	150.9	3.4	0.28
Mesoporous TiO$_2$	130	3.2	0.23
Cu–Mn/TiO$_2$	92.5	2.9	0.10
Mesoporous ZrO$_2$	34.9	3.5	0.11
Cu–Mn/ZrO$_2$	28.5	2.4	0.05

Fig. 2. XRD patterns for mesoporous Al_2O_3 and Cu–Mn/Al_2O_3.
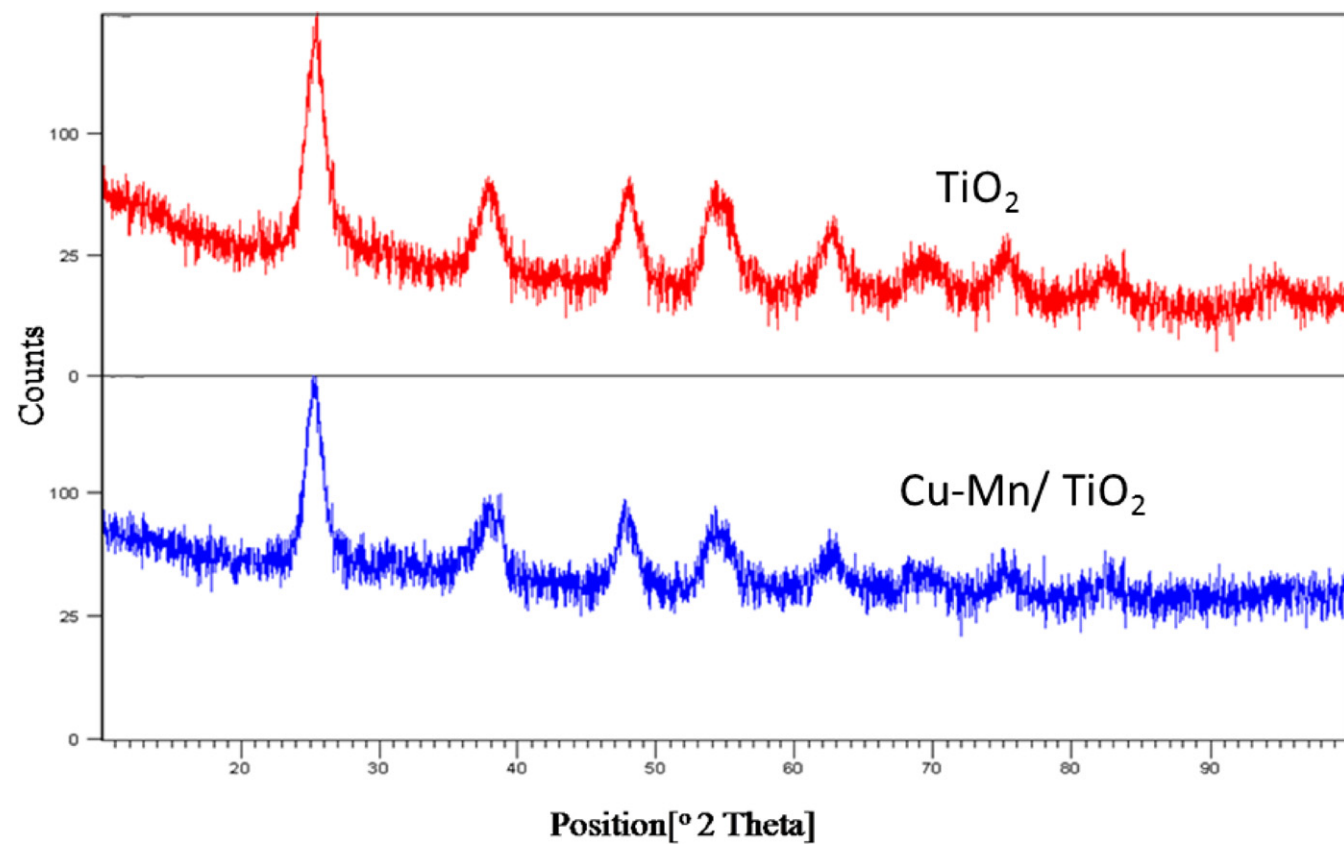

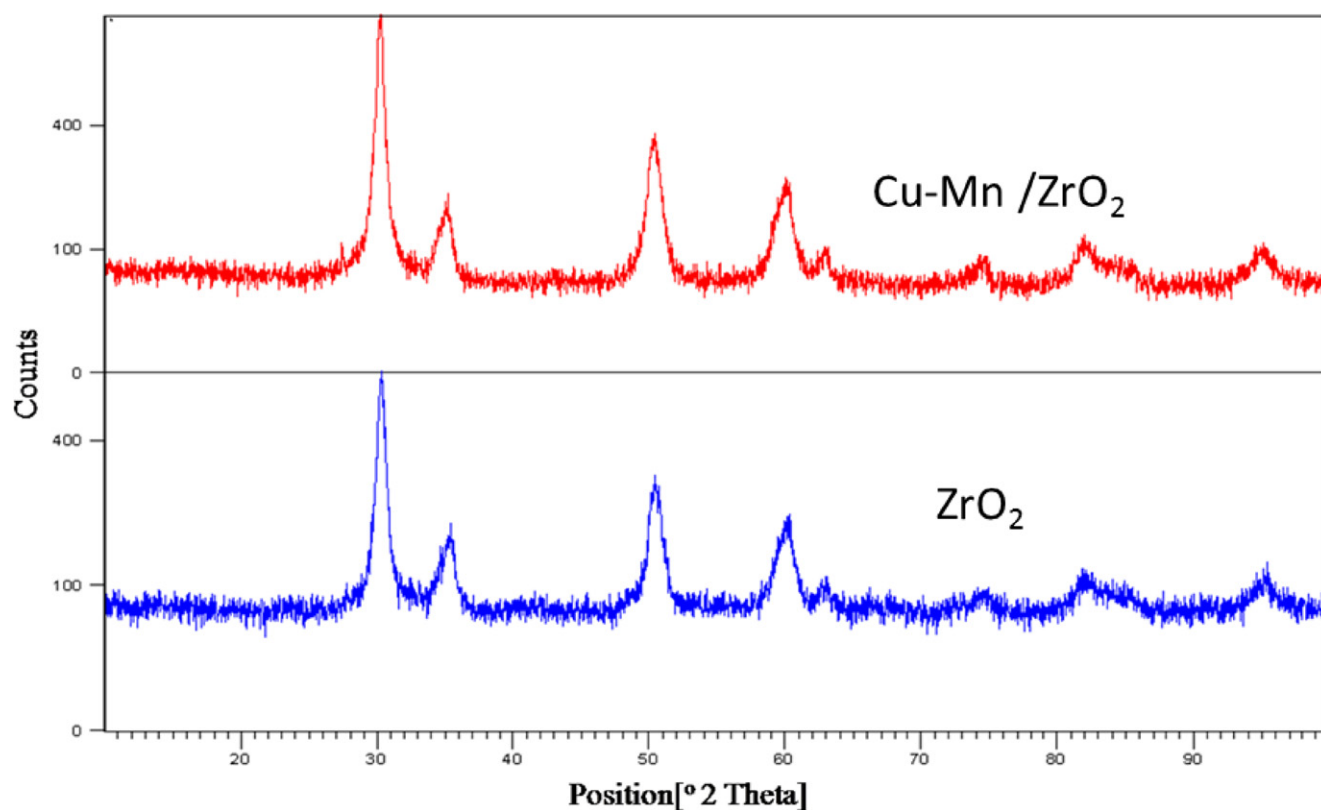**Fig. 3.** XRD patterns for mesoporous TiO_2 and Cu–Mn/TiO_2.

Fig. 4. XRD patterns for mesoporous ZrO_2 and Cu–Mn/ZrO_2.

The highest pore volume was observed for synthesized mesoporous alumina (0.36 cm^3/g) for which, the pore size was utmost followed by titania (0.23 cm^3/g) and zirconia (0.11 cm^3/g). The pore volume of supports has been decreased to 0.28, 0.10 and 0.05 cm^3/g for Al_2O_3, TiO_2 and ZrO_2, respectively after the incorporation of Cu–Mn mixed oxides. This could be due to the formation of mixed oxide crystals on the pores of supports, thereby slightly reducing the pore size and pore volume.

Table 3 presents the CHN analysis results for Cu–Mn/Al_2O_3, Cu–Mn/TiO_2, Cu–Mn/ZrO_2. To conclusively study the presence of chitosan in synthesized Cu–Mn/supported on Al_2O_3, ZrO_2 and TiO_2 samples we have subjected the samples to prolonged heating at 400 °C. On the other hand, we have also heated the samples at 400 °C for longer durations in presence of oxygen. These samples do not show any significant difference in C and N contents, thereby indicating that the chitosan residue is removed almost completely (approx. 99%) at 400 °C.

Although these support materials do not show the ordered structure, the template synthesis results in mesopores with high surface area. These properties result in improved mass transfer and higher number of active sites, important for gas phase catalytic applications. As the target reactions are not shape or size selective reactions, the present supports offer the desired requirements for optimum catalytic activity.

3.1. Catalytic activity measurements

3.1.1. Catalytic activity for benzene decomposition

The catalytic activity results for benzene oxidation as a function of temperature are shown in Fig. 5. The bimetallic supported catalysts follow the activity sequence of Cu–Mn/TiO_2 > Cu–Mn/ZrO_2 > Cu–Mn/Al_2O_3. From Fig. 5, it can be seen that 100% benzene conversion for Cu–Mn/ZrO_2 and Cu–Mn/TiO_2 was observed at 350 °C, whereas, it was observed to be 400 °C for Cu–Mn/Al_2O_3, at approximately 30,000 h^{-1} space velocity. These results suggest that T_i (Temperature at which benzene combustion initiated) and T_{50} (Temperature at
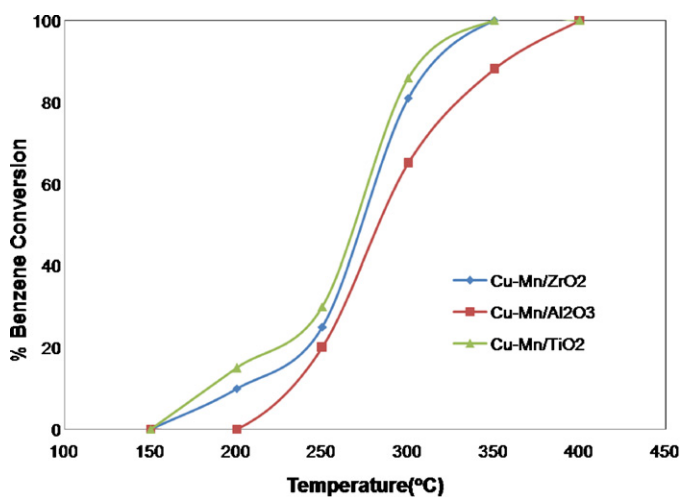
Table 3
Summary of the % CHN of Cu–Mn/Al_2O_3, Cu–Mn/TiO_2, Cu–Mn/ZrO_2.

Sample	%C	%H	%N
Cu–Mn/Al_2O_3	0.58	2.2	0.1
Cu–Mn/TiO_2	0.4	1.1	0.84
Cu–Mn/ZrO_2	0.33	0.9	0.2

Fig. 5. Benzene combustion over Cu–Mn/Al_2O_3, Cu–Mn/TiO_2 and Cu–Mn/ZrO_2 catalysts (feed composition: benzene = 900 ppm, O_2 = 10% balance He, at approximately 30,000 h^{-1} space velocity).

which 50% benzene combustion observed) of Cu–Mn/ZrO$_2$ and Cu–Mn/TiO$_2$ are comparatively lower than that for Cu–Mn/Al$_2$O$_3$. At 200 °C Cu–Mn/Al$_2$O$_3$ shows no activity, whereas Cu–Mn/ZrO$_2$ and Cu–Mn/TiO$_2$ show about 10% and 15% benzene conversion respectively. These results clearly infer that Cu–Mn/TiO$_2$ has enhanced catalytic activity for benzene combustion, followed by Cu–Mn/ZrO$_2$ and Cu–Mn/Al$_2$O$_3$.

Shufeng et al. [31] recently studied the benzene combustion over alumina pillared clay (Al-PILC) supported transition metals (M = Cr, Mn, Fe, Co, Ni and Cu with conditions: catalyst weight 300 mg, benzene concentration = 130–160 ppm composed of air, at 20,000 h^{-1} space velocity). Among the catalysts reported in this work, the 8 wt% Mn supported on Al-PILC shows better catalytic activity as compared to all other catalysts. This catalyst shows 100% benzene conversion at around 390 °C, whereas the present catalysts, Cu–Mn/TiO$_2$ and Cu–Mn/ZrO$_2$ show 100% benzene oxidation at 350 °C, while Cu–Mn/Al$_2$O$_3$ shows 100% benzene conversion at 400 °C. Though the transition metal content in the present study is comparatively high, the high surface area metal oxide incorporated alumina pillared clays (MnO$_2$/Al-PILC and CuO–Al-PILC) studied by Shufeng et al. could also be the possible reason for their superior activity. The evaluation conditions used in the present study are much more severe (benzene concentration is several times higher while space velocity is also one and half times more). Therefore, the catalytic activity of present catalysts is much better. However, Shufeng et al. observed the enhancement of catalytic activity for all the alumina pillared clay (Al-PILC) supported transition metals after promotion with cerium oxide, and the cerium oxide promoted Mn/Al-PILC catalyst reported to show 100% benzene oxidation at about 310 °C. This can be explained based on the well known fact of oxygen storage capacity of cerium oxide. However, even this catalytic activity can be well compared with the present results (100% benzene oxidation at 350 °C) considering the above mentioned evaluation conditions.

The activity of the investigated catalysts has also been compared with some of the recently reported noble metal based catalysts. Nedyalkova et al. studied the catalytic activity of gold catalysts supported on titania and ceria for complete benzene oxidation (CBO). In that study the authors studied the benzene oxidation under the following conditions: catalyst weight 500 mg, benzene concentration 4.2 ppm and space velocity 40,000 h^{-1}. Au/CeO$_2$ and Au/TiO$_2$ catalysts investigated by Nedyalkova et al. start showing benzene conversion at around 150 °C and complete oxidation of benzene was observed at around 260 °C. The activity of the catalysts studied in the present research can be considered as much improved activity as high concentration of benzene (900 ppm) and small amount of catalyst (100 mg) were used to investigate the catalysts [32]. Shufeng et al. also studied the 0.2 wt% palladium supported alumina pillared clays for the complete oxidation of low concentration of benzene. In this study, the authors have carried out the benzene oxidation in the following conditions: catalyst (300 mg), benzene (130–160 ppm), reactive flow (125 ml/min), space velocity of 20,000 h^{-1}. The authors observed 100% benzene conversion for 0.2 wt% palladium supported alumina pillared clays at 360 °C. Although the reactive flow of the present study is low (50 ml/min), considering small amount of catalyst (100 mg), the space velocity used in the present study is 30,000 h^{-1} which is considerably higher in addition to several times higher concentration of benzene. This reflects in overall much higher amount of benzene oxidation and confirms superior activity of Cu–Mn/TiO$_2$ in comparison with the reported work of Shufeng et al. [33].

3.1.2. Catalytic activity for acetaldehyde decomposition

The Cu–Mn/Al$_2$O$_3$, Cu–Mn/ZrO$_2$ and Cu–Mn/TiO$_2$ catalysts have also been evaluated for their activity towards catalytic acetaldehyde oxidation, as acetaldehydes are among
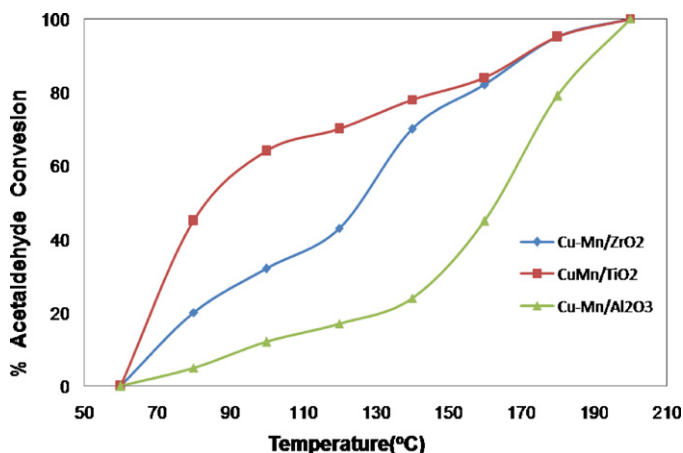

Fig. 6. Acetaldehyde combustion over Cu–Mn/Al$_2$O$_3$, Cu–Mn/TiO$_2$ and Cu–Mn/ZrO$_2$ (feed composition: acetaldehyde = 500 ppm, O$_2$ = 10% balance He, at approximately 30,000 h^{-1} space velocity).

the most common VOC pollutants in indoor air. Fig. 6 shows the acetaldehyde decomposition over Cu–Mn/Al$_2$O$_3$, Cu–Mn/ZrO$_2$ and Cu–Mn/TiO$_2$ catalysts. The same activity sequence (Cu–Mn/TiO$_2$ > Cu–Mn/ZrO$_2$ > Cu–Mn/Al$_2$O$_3$) was also observed in case of acetaldehyde oxidation. The Cu–Mn/Al$_2$O$_3$, Cu–Mn/TiO$_2$ and Cu–Mn/ZrO$_2$ catalysts get activated after about 60 °C and quickly achieve the light-off temperature. 100% decomposition of acetaldehyde for all the catalysts was obtained at about 200 °C at 30,000 h^{-1} space velocity. The T_i (temperature at which acetaldehyde combustion initiated) and T_{50} (temperature at which 50% acetaldehyde combustion observed) of Cu–Mn/ZrO$_2$ and Cu–Mn/TiO$_2$ are comparatively lower than that for Cu–Mn/Al$_2$O$_3$. At 80 °C, Cu–Mn/Al$_2$O$_3$ shows 5% acetaldehyde conversion, whereas Cu–Mn/ZrO$_2$ and Cu–Mn/TiO$_2$ show 20% and 45% acetaldehyde conversion, respectively.

The catalytic abatement of acetaldehyde over non-noble metal based catalyst is not frequently reported, therefore the present results were compared with works of Mitsui et al. [34], in which the authors have studied the catalytic combustion of acetaldehyde over SiO$_2$, TiO$_2$ and CeO$_2$ supported 1 wt% Pt catalysts. A gaseous mixture of 1% acetaldehyde and 99% air was used in the study, and the catalysts were evaluated at 10,000 h^{-1} space velocity using 600 mg of catalyst. All the investigated 1 w% Pt supported SiO$_2$, TiO$_2$ and CeO$_2$ catalysts show 100% acetaldehyde conversion at 250 °C. The Cu–Mn/Al$_2$O$_3$, Cu–Mn/ZrO$_2$ and Cu–Mn/TiO$_2$ catalysts studied in the present work (Fig. 6) show the 100% acetaldehyde conversion at 200 °C. Although, lower acetaldehyde concentration was used in the present work as compared to the studies of Mitsui et al., considering the small amount of catalyst (100 mg) and higher space velocity (30,000 h^{-1}) used in the present investigation, these non-noble metal catalysts show excellent activity for the combustion of acetaldehyde.

It has been reported that alumina usually forms less active aluminates with the transition metals, which could be the possible reason for the inferior activity of Cu–Mn/Al$_2$O$_3$ catalyst [35]. The redox and oxygen desorption properties of TiO$_2$ and ZrO$_2$ prevent the formation of titanates and zirconates with Cu and Mn under the present synthesis conditions used [36]. In this way, Al$_2$O$_3$ shows inferior catalytic activity as compared to TiO$_2$ and ZrO$_2$, when used as support for the transition metals, unlike in the case of noble metals like Pt and Pd, which are not reactive towards alumina. The use of acidic supports and catalysts for the removal of various pollutants is well established for many catalytic reactions of energy and environmental importance. Tajima et al. [37] studied the decomposition of chlorofluorocarbons on different acidic supports such
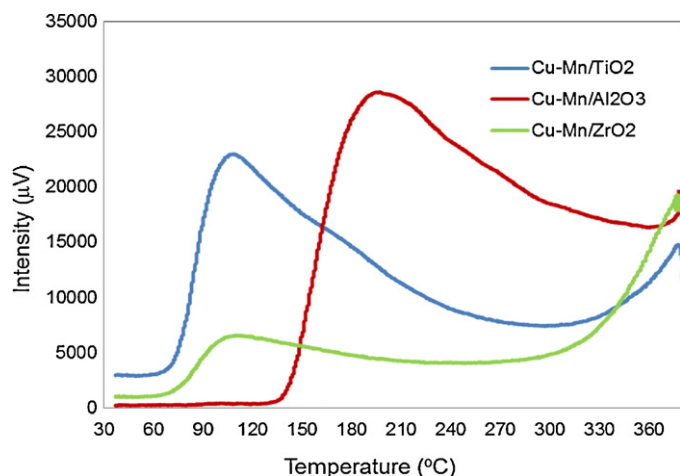
Fig. 7. O_2-TPD curves for Cu–Mn/Al$_2$O$_3$, Cu–Mn/TiO$_2$ and Cu–Mn/ZrO$_2$.

Fig. 8. H_2-TPR curves for Cu–Mn/Al$_2$O$_3$, Cu–Mn/TiO$_2$ and Cu–Mn/ZrO$_2$.

as SiO$_2$–MgO, SiO$_2$–ZrO$_2$, SiO$_2$–Al$_2$O$_3$ and TiO$_2$–ZrO$_2$. Among the studied catalysts only TiO$_2$–ZrO$_2$ catalysts show enhanced activity, though the other catalyst studied were also of acidic nature.

Clearly the present work infers that TiO$_2$ and ZrO$_2$ are better supports for transition metal based oxide and mixed oxide type catalysts and their physical properties can be significantly enhanced through template synthesis.

3.2. O_2-TPD studies

O_2-TPD (temperature programmed oxygen desorption) experiments were performed to understand the oxygen desorption properties of Cu–Mn/Al$_2$O$_3$, Cu–Mn/ZrO$_2$ and Cu–Mn/TiO$_2$. Two different types of oxygen species known as α and β were defined in our previous O$_2$-TPD studies on mixed oxide materials for soot oxidation reaction [38]. The peaks at low temperatures are supposed to be desorbed α oxygen species, which are weakly chemisorbed superficial oxygen species. Fig. 7 shows the O$_2$-TPD curves for Cu–Mn/Al$_2$O$_3$, Cu–Mn/TiO$_2$ and Cu–Mn/ZrO$_2$. The α-oxygen desorption temperatures are observed around 180, 135 and 120 °C for Cu–Mn/Al$_2$O$_3$, Cu–Mn/TiO$_2$ and Cu–Mn/ZrO$_2$, respectively. The lower temperature α-oxygen desorption further support the better catalytic activity results for Cu–Mn impregnated ZrO$_2$ and TiO$_2$ as compared to Cu–Mn impregnated Al$_2$O$_3$. The high activity of Cu–Mn/TiO$_2$ catalyst also correlates very well with the oxygen species of peak α, i.e. larger area of peak α corresponds to higher combustion activity of the catalyst. From the results it can also be seen that α oxygen releasing temperature of the Cu–Mn/ZrO$_2$ is low, which represents the oxygen desorption properties of Cu–Mn/ZrO$_2$ at lower temperatures as compared to Cu–Mn/TiO$_2$. However, the smaller surface area of this catalyst could also be responsible for smaller α oxygen content of this catalyst. Hence this catalyst shows slightly inferior activity than that of Cu–Mn/TiO$_2$. The catalyst support interaction leading to improved redox properties is the likely cause for the enhanced catalytic activity of Cu–Mn/TiO$_2$ and Cu–Mn/ZrO$_2$.

3.3. H_2-TPR studies

Fig. 8 depicts the H$_2$-TPR (temperature programmed reduction with hydrogen) profiles of Cu–Mn/Al$_2$O$_3$, Cu–Mn/TiO$_2$ and Cu–Mn/ZrO$_2$ catalysts. The obtained H$_2$-TPR profiles show two reduction peaks for Cu–Mn/TiO$_2$ and Cu–Mn/ZrO$_2$, whereas Cu–Mn/Al$_2$O$_3$ shows the single reduction peak. It has been reported that the low temperature peak/peaks is/are due to highly dispersed metal oxide particles on supports and the second reduction peak
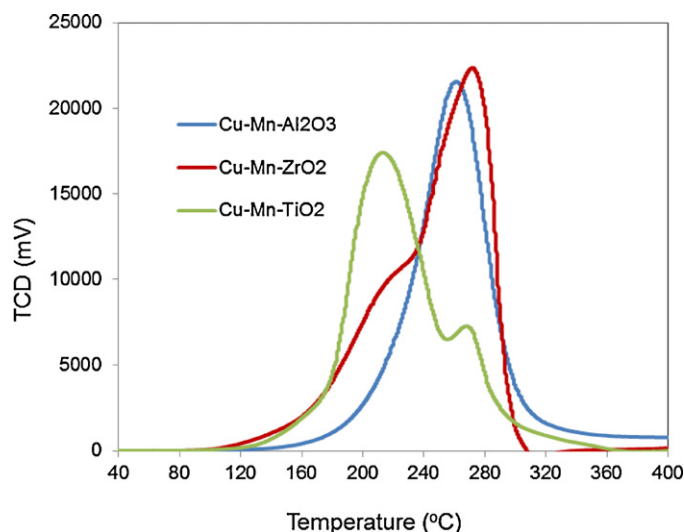
is usually assigned to the hydrogen consumed in the reaction with sub-surface lattice oxygen, which can be migrated at higher temperatures from the interior to the surface of the catalyst [39,40]. From the present H$_2$-TPR results, it is clear that Cu–Mn/TiO$_2$ catalyst is easily reduced followed by Cu–Mn/ZrO$_2$ and Cu–Mn/Al$_2$O$_3$. It has been observed in many studies that the increasing order of catalyst reduction ability can be correlated to their redox ability [40]. Hence the better performance of Cu–Mn/TiO$_2$ catalyst at relatively lower temperatures could be explained by the ease of reducibility of this catalyst in comparison with Cu–Mn/ZrO$_2$ and Cu–Mn/Al$_2$O$_3$. The H$_2$-TPR curves in the temperature range of catalytic activity can be further correlated to the better catalytic performances of the investigated catalysts.

4. Conclusion

The results obtained in the present study for the catalytic benzene and acetaldehyde combustion, clearly suggest that Al$_2$O$_3$, TiO$_2$ and ZrO$_2$ are the potential supports for catalyst dispersion. The mesoporous nature of these supports without ordered structure offer suitable properties for dispersion of metal oxides and mixed metal oxides. The higher surface area and open type pore structure with mesoporous size are observed to be very suitable for reactions involving VOCs molecules, which could be mainly due to the improved mass transfer. The redox properties of TiO$_2$ and ZrO$_2$ could be the possible reasons for the better catalytic activity of Cu–Mn/TiO$_2$ and Cu–Mn/ZrO$_2$ catalysts as compared to Cu–Mn/Al$_2$O$_3$ for both combustion of benzene and acetaldehyde. TPD and TPR experiments further support the enhanced activity of Cu–Mn/TiO$_2$ through its redox properties. The effect of oxygen, benzene and acetaldehyde concentration on catalytic performance will be investigated in the subsequent work. The most striking observation of the present catalysts is the possibility of development of low cost catalyst compositions as a replacement of those noble metals. The development of catalyst supports with improved properties is a significant advancement in this respect.

References

[1] H.H. Kim, A. Ogata, Int. J. Plasma Environ. Sci. Technol. 1 (2007) 46–51.
[2] F.I. Khan, A.K. Ghosal, J. Loss Prev. Process Indust. 13 (2000) 527–545.
[3] E. Noordally, J.R. Richmond, S.F. Tahir, Catal. Today 17 (1993) 359–366.
[4] K.J. Kim, H.G. Ahn, Carbon 48 (2010) 2198–2202.
[5] G.J. Dollard, P. Dumitrean, P. Kent, Atmos. Environ. 37 (2003) 1983–1999.
[6] H.H. Kim, A. Ogata, S. Futamura, Environ. Sci. Technol. 1 (1) (2007) 46–51.
[7] H. Einaga, A. Ogata, Environ. Sci. Technol. 44 (2010) 2612–2617.
[8] A. Gervasini, G.C. Vezzoli, V. Ragaini, Catal. Today 29 (1996) 449–455.
[9] S. Ojala, U. Lassi, R. Ylonen, R. Keiski, I. Laakso, T. Maunula Silvonen, Tappi J. 4 (2005) 9–14.
[10] R. Prasad, L.A. Kennedy, E. Ruckenstein, Catal. Rev. Sci. Eng. 26 (1984) 1–58.
[11] M.R. Morales, B.P. Barbero, L.E. Cadus, Fuel 87 (2008) 1177–1186.
[12] M. Zimowska, Z.A. Michalik, R. Janik, T. Machej, J. GurgulR., P. Socha, J. Podobinski, E.M. Serwicka, Catal. Today 119 (2007) 321–332.
[13] M.R. Morales, B.P. Barbero, L.E. Cadus, Appl. Catal. B 67 (2006) 229–236.
[14] Q. Liang, X. Wu, D. Weng, H. Xu, Catal. Today 139 (2008) 113–118.
[15] X. Du, Z. Yuan, L. Cao, C. Zhang, S. Wang, Fuel Process. Technol. 89 (2008) 131–138.
[16] H. Rogers, C.S. Piggot, W.H. Bahlke, J.M. Jennings, J. Am. Chem. Soc. 43 (1921) 1973.
[17] H.A. Jones, H.S. Taylor, J. Phys. Chem. 27 (1923) 623.
[18] J.Christoper, J.C. Kiren, S.H. Taylor, J.C. Mandy, J.H. Hutcings, J. Mol. Catal. A 305 (2009) 121–124.
[19] W.B. Li, M. Zhuang, J.X. Wang, Catal. Today 137 (2008) 340–344.
[20] N.F. Aguero, P.B. Barbero, L. Gambaro, E.C. Luis, Appl. Catal. B 91 (2009) 108–112.
[21] E.M. Cordi, P.J. Neill, P.O.L. Falconer, Appl. Catal. B 14 (1997) 23–36.
[22] M.M. Yung, E.M. Holmgreen, U.S. Ozkan, J. Catal. 247 (2007) 356–367.
[23] J. Rasko, J. Kiss, Appl. Catal. A 287 (2005) 252–260.
[24] H.V. Van, J. Belkouch, D.A. Ould, B. Taouk, J. Hazard. Mater. 169 (2009) 758–765.
[25] C. Bozo, N. Guilhaume, J.M. Herrmann, J. Catal. 203 (2001) 393–406.
[26] G.L Markaryan, L.N. Ikryannikova, G.P. Muravieva, A.O. Turakulova, B.G. Kostyuk, E.V. Lunina, V.V. Lunin, E.A. Zhilinskaya, A. Aboukaıs, Colloids Surf. A 151 (1999) 435–447.
[27] D. Thakre, S. Jagtap, N. Sakhare, N. Labhsetwar, S. Meshram, S. Rayalu, Chem. Eng. J. 129 (2009) 173–180.
[28] P. Doggali, H. Kusaba, H. Einaga, S. Bensaid, S. Rayalu, Y. Teraoka, J. Hazard. Mater. 186 (2010) 796–804.
[29] H.V Fajardo, A.O. Martins, R.M. de Almeida, L.K. Noda, L.F.D. Probst, N.L.V. carreno, A. Valentini, Mater. Lett. 59 (2005) 3963–3967.
[30] M. Joshi, N.K. Labhsetwar, P.A. Mangrulkar, S.N. Tijare, S.P. Kamble, S.S. Rayalu, Appl. Catal. A 357 (2009) 26–33.
[31] Z. Shufeng, H. Quinquin, L. Jing, Z. Renxian, Appl. Catal. B 91 (2009) 204–209.
[32] R. Nedyalkova, L. Ilieva, M.C. Bernard, A.H. Goff, D. Andreeva, Mater. Chem. Phys. 116 (2009) 214–218.
[33] Z. Shufeng, Z. Renxian, Q. Chenze, J. Rare Earths 29 (2011) 52–57.
[34] T. Mitsui, T. Kazuki, M. Toshiaki, K. Ryuji, E. Koichi, Appl. Catal. B 78 (2008) 158–165.
[35] G.Aguila, F. Gracia, P. Araya, Appl. Catal. A 343 (2008) 16–24.
[36] W. Dow, T. Huang, J. Catal. 147 (1994) 322–332.
[37] M. Tajima, M. Niwa, Y. Fujii, Y. Koinuma, R. Aizawa, S. Kushiyama, S. Kobayashi, K. Mizuno, H. OhGchi, Appl. Catal. B 12 (1997) 263–276.
[38] M. Dhakad, N.K. Labhsetwar, S.S. Rayalu, R. Kumar, P. Doggali, S. Bakardjieva, J. Subrt, T. Mitsuhashi, H. Haneda, Catal. Lett. 121 (2008) 137–143.
[39] J. Lamonier, M. Labaki, F. Wyrwalski, S. Siffert, A. Aboukais, J. Anal. Appl. Pyrol. 81 (2008) 20–26.
[40] M. Shimokawabe, H. Asakawa, N. Takezawa, Appl. Catal. B 59 (1990) 45–49.